

1                    BiœmuS: A new tool for neurological  
2                    disorders studies through real-time emulation  
3                    and hybridization using biomimetic Spiking  
4                    Neural Network

5                    Romain Beaubois<sup>1,2\*</sup>, Jérémie Cheslet<sup>1,2</sup>, Tomoya  
6                    Duenki<sup>2,3,4</sup>, Farad Khoyratee<sup>1</sup>, Pascal Branchereau<sup>5</sup>, Yoshihiro  
7                    Ikeuchi<sup>2,4,6</sup> and Timothée Lévi<sup>1\*</sup>

8                    <sup>1</sup>\*IMS Laboratory UMR5218, University of Bordeaux France.

9                    <sup>2</sup>LIMMS, CNRS-Institute of Industrial Science, UMI 2820, The  
10                    University of Tokyo, Japan.

11                    <sup>3</sup>Department of Chemistry and Biotechnology, Graduate School  
12                    of Engineering, The University of Tokyo, Japan.

13                    <sup>4</sup>Institute of Industrial Science, The University of Tokyo, Japan.

14                    <sup>5</sup>INCIA, UMR5287, CNRS, University of Bordeaux, France.

15                    <sup>6</sup>Institute for AI and Beyond, The University of Tokyo, Japan.

16                    \*Corresponding author(s). E-mail(s):  
17                    [romain.beaubois@u-bordeaux.fr](mailto:romain.beaubois@u-bordeaux.fr); [timothee.levi@u-bordeaux.fr](mailto:timothee.levi@u-bordeaux.fr);  
18                    Contributing authors: [jeremy.cheslet@u-bordeaux.fr](mailto:jeremy.cheslet@u-bordeaux.fr);  
19                    [tomoyaduenki@g.ecc.u-tokyo.ac.jp](mailto:tomoyaduenki@g.ecc.u-tokyo.ac.jp); [farad.khoyratee@gmail.com](mailto:farad.khoyratee@gmail.com);  
20                    [pascal.branchereau@u-bordeaux.fr](mailto:pascal.branchereau@u-bordeaux.fr); [yikeuchi@iis.u-tokyo.ac.jp](mailto:yikeuchi@iis.u-tokyo.ac.jp);

21                    **Abstract**

22                    Characterization and modeling of biological neural networks  
23                    has emerged as a field driving significant advancements in  
24                    our understanding of brain function and related pathologies.  
25                    As of today, pharmacological treatments for neurological dis-  
26                    orders remain limited, pushing the exploration of promising  
27                    alternative approaches such as electroceutics. Recent research  
28                    in bioelectronics and neuromorphic engineering have led to the  
29                    design of the new generation of neuroprostheses for brain repair.

30 However, its complete development requires deeper understanding  
31 and expertise in biohybrid interaction. Here, we show a  
32 novel real-time, biomimetic, cost-effective and user-friendly neural  
33 network for bio-hybrid experiments and real-time emulation.  
34 Our system allows investigation and reproduction of biophysically  
35 detailed neural network dynamics while promoting cost-efficiency, flex-  
36 ibility and ease of use. We showcase the feasibility of conducting  
37 biohybrid experiments using standard biophysical interfaces and various  
38 biological cells as well as real-time emulation of complex models.  
39 We anticipate our system to be a step towards developing neuromorphic-  
40 based neuroprostheses for bioelectrical therapeutics by enabling com-  
41 munication with biological networks on a similar time scale, facili-  
42 tated by an easy-to-use and accessible embedded real-time system.  
43 Our real-time device further enhances its potential  
44 for practical applications in biohybrid experiments.

45 **Keywords:** Real time, FPGA, SNN, Bio hybrid, Hodgkin Huxley

## 46 1 Introduction

47 Millions of people worldwide are affected by neurological disorders that  
48 strongly impair their cognitive and/or motor functions [1]. An increasing num-  
49 ber of technologies and solutions are currently proposed for the treatments  
50 of these diseases, whereas being limited to curbing the progress or managing  
51 symptoms in most cases [2, 3].

52 Aside from medical treatment through chemical processes, artificial devices  
53 are developed to improve the quality of life of individuals. To bring neuro-  
54 prosthesis into realization, the behavior of biological neurons as well as its  
55 connection and interaction with artificial neural networks must be consid-  
56 ered. To this end, investigation of the interaction of neuronal cell assemblies is  
57 required to understand and reproduce a specific behavior driven by intrinsic  
58 spontaneous activity. Additionally, long-term replacement of damaged brain  
59 areas with artificial devices implies understanding of their neurophysiological  
60 behaviors.

61 In this context, new therapeutic approaches and technologies are needed  
62 both to promote cell survival and regeneration of local circuits [4] and restore  
63 long distance communication between disconnected brain regions and circuits  
64 [5]. Thus, characterization and modeling of biological neural networks [6, 7]  
65 is crucial to develop new generation of neuroprostheses that mimics biological  
66 dynamics and provide adaptive stimulation at biological time scale based on  
67 the principle of electroceutics [8, 9].

68 Thanks to the new neuromorphic platforms, performing bio-hybrid exper-  
69 iments is becoming more and more relevant not only for the development of  
70 neuromorphic biomedical devices [8, 9], but also to elucidate the mechanisms  
71 of information processing in the nervous system. Recently, major progress has

been made in the field of neuroprostheses [6, 7] so as neuromorphic devices are now capable of receiving and processing input while locally or remotely delivering their output either through electrical, chemical or optogenetic stimulation [10].

However, real-time stimulation and processing of biological data using biomimetic Spiking Neural Network (SNN) is still quite rare [11]. Furthermore, to improve temporal accuracy of the stimulation, complex neuron model should be implemented in the SNN [12].

To perform bi-directional bio-hybrid experiments and develop bioelectrical therapeutic solutions for health care like electroceutic [8, 9, 13], real-time bio-physics interface and SNN processing are mandatory to ensure interaction at biological time scale [12, 14]. Most of current solutions for biomimetic SNN simulations are software-based such as NEURON [15], NEST [16] or Brian2 [17] tools and show significantly high computation time, especially for complex neuron model with synaptic plasticity. Hence, these latter are not suited for real-time emulation at millisecond time step [18] contrary to hardware-based SNNs. Another benefit of hardware-based SNNs is the ability to perform massive parallel simulations to explore space parameters of neuron models.

In the neuromorphic engineering research, SNNs are designed using two distinct approaches: bioinspired or biomimetic. The former is widely used for applications such as computation and artificial intelligence [19] using accelerated time simulation of simple neuron model. The latter uses complex neuron model operating at biological time scale to simulate neural network dynamics or/and performing bio-hybrid experiments.

Hardware-based SNNs are analog or digital. Analog SNN systems [20] show lower power consumption than digital SNNs [21]. In contrast, digital SNNs are more flexible thus more suited for prototyping while showing overall quicker design time hence constituting the best choice for preliminary experiments and design of new generation of neuroprosthetic. The prominent SNNs hardware platforms are Merolla [22], BrainScaleS-2 [23], SpiNNaker [24] and Loihi [25]. While some of these systems present mobile versions like [26] for BrainScaleS-2, they often are not suited for embedded applications. In this manuscript, we present the capabilities of the real-time biomimetic SNN BioemuS to emulate independent neurons and fully connected networks, showcasing a system integration promoting versatility and ease of use.

## 2 Results

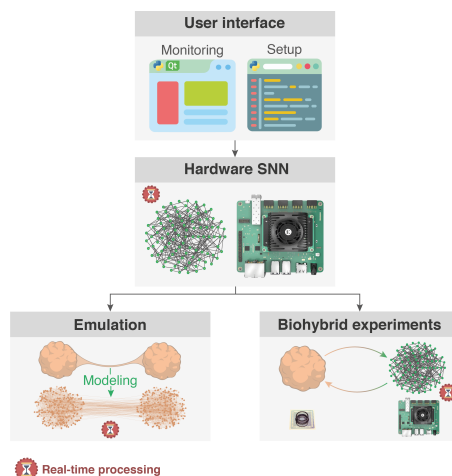
### 2.1 Real-time biomimetic SNN

The low-cost platform targeted is based on a System on Chip (SoC) featuring both Programmable Logic (PL, i.e. FPGA) and processors in a Processing System (PS) part. It is capable of running up to 1,024 neurons fully connected, supporting a total of  $2^{20}$  synapses. It includes on-board monitoring and offers versatile external communication options such as Ethernet, WiFi, expansion PMODs (standard peripheral module interface) and a Raspberry Pi header.

113 4

114

115 The system is used either for real-time emulation as a low-cost computing unit  
116 or for biohybrid experiments thanks to its versatility (see Figure 1).

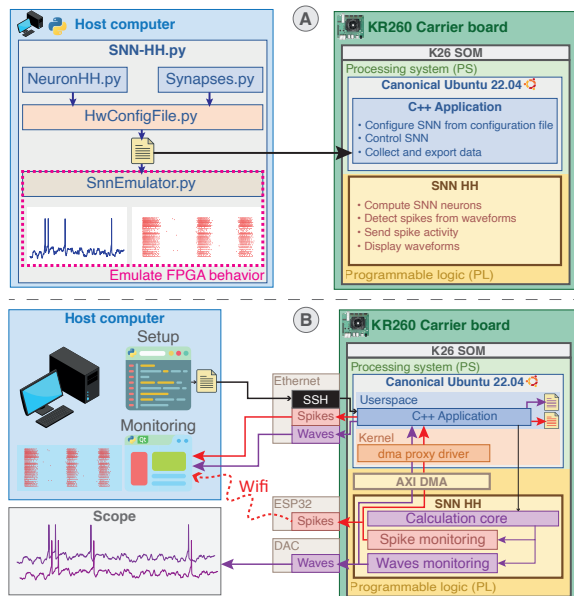


117

118 **Fig. 1** Overview of system applications. The real-time biomimetic SNN implemented in  
119 hardware is monitored through a Qt-based GUI and setup by Python scripts ran either  
120 on-board or on another computer. The SNN is used either as a real-time emulator for biophysically  
121 realistic models or integrated in a biohybrid experiment setup. In a real-time emulation  
122 setup, it runs fast simulations of biophysically detailed models suited for large parameters  
123 sweeps. Integrated in a biohybrid experimental setup, it acts as a versatile biomimetic artificial  
124 neural network easily interfaced with standard biological recording units.

### 136 2.1.1 Independents neurons

137 The neurons composing the SNN are modeled with high biological plausibility  
138 using the Hodgkin-Huxley (HH) paradigm [27] in the Pospichil model [28]  
139 implementing 6 conductance-based currents. An injected current mimicking  
140 synaptic noise following an Ornstein–Uhlenbeck process [29, 30] reproduces  
141 spontaneous activity by triggering action potentials on a random basis. All  
142 parameters of the HH model as well as the synaptic noise parameters are tuned  
143 through the 25 parameters available from the Python scripts (see Figure 2A).  
144 The scripts implements 4 preset neuron types including Fast Spiking (FS),  
145 Regular Spiking (RS), Intrinsic Burst (IB) and Low Threshold Spiking (LTS)  
146 neurons and allow the user to create new presets. The equations of ionic chan-  
147 nel states are pre-computed and stored in memory so that they can be easily  
148 modified to any channel dynamic without impact on the performances of the  
149 system or limitations on mathematical functions used. The computation of  
150 ionic currents is performed using 32 bits floating point coding allowing emula-  
151 tion of currents with different dynamics potentially smaller in comparison to  
152 other currents like for  $\text{Ca}^{2+}$ -based current in IB or LTS neurons.



125

126 **Fig. 2** Complete system architecture and integration. (A) Overview of system setup from  
127 the configuration file generated by Python scripts ran either on-board or on another computer.  
128 The configuration file is then read by a C++ application running on Canonical Ubuntu  
129 operating system in the Processing System (PS) part to set up the SNN in Programmable  
130 Logic (PL) part. Configuration can be emulated beforehand to predict the behavior. (B)  
131 Schematic of system communication. System control is achieved through the C++ application  
132 either remotely *via* SSH or directly on-board from the Ubuntu desktop. Spikes can  
133 be monitored concurrently using Ethernet, WIFI and on-board file saving. Waveforms can  
134 be monitored concurrently using Ethernet, visualization on scope by probing the Digital-to-  
135 Analog Converter (DAC) and on-board file saving.

### 153 2.1.2 Connected network

154 Neurons are connected using biomimetic synapses mimicking AMPA, NMDA,  
155 GABA<sub>A</sub> and GABA<sub>B</sub> receptors [31] to allow fast and slow synaptic excitation  
156 or inhibition, computed using 18 bits fixed point coding. The parameters  
157 of the synaptic models can be tuned similarly to the HH parameters through  
158 the Python scripts (see Figure 2A). Synaptic connection can be established  
159 between all neurons and independently weighted using the Python script allowing  
160 the user to create custom functions to setup the connections. The generated  
161 configuration file can be emulated using the Python scripts to assess behavior  
162 and verify membrane voltage, ionic channel state equations, internal variables  
163 and raster plot (see Figure 2A).

### 164 2.1.3 Monitoring interface

To maximize compatibility and versatility, a Canonical Ubuntu is running on the processors of the board. Compatibility and versatility are important

165 6

166

167 criteria, knowing that standards for communication protocol interfacing bio-  
168 logical recording units vary along with manufacturers (e.g., Serial Peripheral  
169 Interface (SPI), Ethernet, USB). In addition, laboratories often have custom  
170 setup, designed to reach their specific needs or inherited from prior experi-  
171 mental settings. The selected carrier board features notably multiple USB3.0  
172 and Ethernet ports as well as expansion PMODs (standard peripheral module  
173 interface) and Raspberry Pi headers.

174 The on-board monitoring allows to store all spikes and up to 16 waveforms  
175 in a file or/and forward it through ZeroMQ (see Figure 2B). Up to 8 membrane  
176 voltage of neurons are selected at a time and output per Digital-to-Analog  
177 Converter (DAC) plugged on PMOD connectors. Data is moved from the PL  
178 to PS using Direct Memory Access (DMA) interfaced by Advanced eXtensible  
179 Interface (AXI) using a driver, thus providing high throughput and good scal-  
180 ing. The interval of collection and forwarding for spikes and waveforms can be  
181 set from the application settings.

182 A wireless setup communication for embedded applications is also provided  
183 via WiFi using a PMOD ESP32 that plugs on PMOD connectors for spike  
184 monitoring. It communicates directly to the PL via SPI protocol driven by  
185 an ESP32 micro-controller that is able to receive and send data through WiFi  
186 network (see Figure 2B). This solution offers a more flexible approach for  
187 interconnection of the system that suit well in-vivo applications where cables  
188 are a concern, while maintaining a low latency and acceptable throughput. In  
189 addition, this constitutes a reusable element to build a reduced and minimal  
190 embedded version of the system targeting a smaller programmable logic only  
191 target to create an energy-efficient solution for embedded applications.

## 192 2.1.4 System control

193 The SNN is setup from the configuration file generated by Python scripts  
194 (see Figure 2A) that is either generated directly on-board using the python  
195 installed on the Ubuntu operating system or prior on another computer. The  
196 application controlling the system is launched directly using the Ubuntu desk-  
197 top on the board or remotely over SSH (see Figure 2B). The parameters of  
198 the application are generated to JSON format along with the configuration file  
199 so as the user may apply changes without code recompilation. The parame-  
200 ters allows to setup the addresses for ZeroMQ forwarding, the local saving or  
201 other parameters such as the neurons to monitor. The firmware can be easily  
202 updated and loaded by running bash scripts, allowing convenient management  
203 of alternative versions developed for a custom dedicated hardware. An external  
204 stimulation trigger for each neuron with an independent duration is available  
205 via ZeroMQ to easily integrate the system in closed-loop setups.

## 206 2.2 Real-time emulation

207 This section demonstrates two applications that use BioemuS as a real-time  
208 emulator of biomimetic networks to create a fast emulation setup for large  
209 biophysically detailed network.

### 210 2.2.1 Interconnected organoids emulation

211 A more complex network model is emulated representing three-dimensional  
212 tissue cultures that are derived from stem cells known as cortical organoids  
213 and their interconnections. This model introduces three types of structures  
214 promoting different synaptic connections between two organoids as illustrated  
215 in Figure 3A.

216 The structure named "single" physically separates the organoids to prevent  
217 connection between organoids. It acts as a reference model showing activi-  
218 ty of independents organoids. The "assembloid" or fused structure places  
219 organoids close to each other thus favouring connection of neurons based on  
220 proximity [32]. The "connectoid" structure places organoids centimeters apart  
221 while constraining the interconnection to form an axon bundle connecting  
222 mostly neurons on the surface of the organoid [33, 34]. The parameters of  
223 the SNN were tuned to match the electrical activity in terms of mean fir-  
224 ing, synchronicity and burst activity of each structure obtained from MEA  
225 recordings.

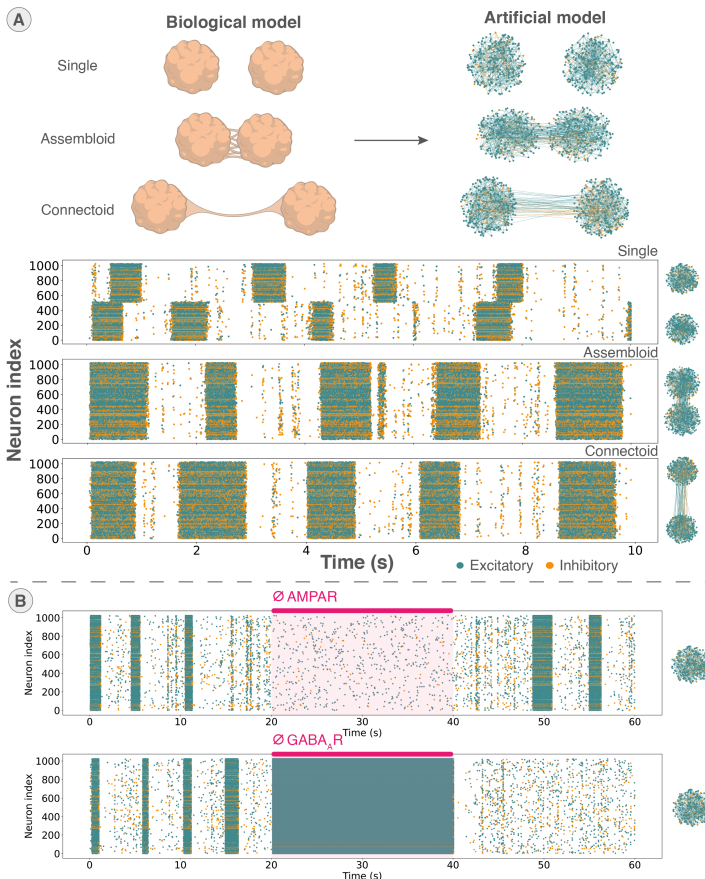
226 An additional Python class has been created for that specific model case to  
227 assign normally distributed XY coordinates to neurons and generate synaptic  
228 connections based on specific rules for each structure. The matrix of connec-  
229 tion and list of neurons generated is then simply translated to hardware SNN  
230 configuration by the existing software (see Figure 2A), showcasing a case of  
231 custom user script to generate the network structure.

232 The three structures were emulated using 1,024 neurons distributed equally  
233 between the two organoids with a similar inhibitory/excitatory ratio to biol-  
234 ogy. Inhibition is modeled using FS neurons connecting by GABA<sub>AR</sub> and  
235 excitation by RS neurons connecting by AMPAR. The emulation is able to  
236 reproduce from network bursts to burst synchronization between organoids in  
237 the assembloid and connectoid structures as shown in Figure 3A.

### 238 2.2.2 Drug treatments emulation

239 An example of application is the emulation of drug treatments targeting synap-  
240 tic receptors in an organoid. Two emulations were performed to reproduce  
241 a treatment by full antagonist of AMPAR (CNQX) and a treatment by full  
242 antagonist to GABA<sub>AR</sub> (Bicuculine). An organoid of similar structure as pre-  
243 viously presented is modeled using 1,024 FS and RS neurons connecting with  
244 AMPAR and GABA<sub>AR</sub> is emulated on BioemuS. During emulation, a trigger  
245 is sent to BioemuS to disable a given receptor thus mimicking the drug treat-  
246 ment by full antagonist and a second trigger is sent to reactivate the receptor  
247 (see Figure 3B).

248 We show that the system emulates coherent behavior since the full antag-  
249 onist to AMPAR prevents bursting and desynchronizes the activity while the  
250 full antagonist to GABA<sub>AR</sub> generates continuous spiking activity similar to  
251 an epilepsy (see Figure 3B).



253 **Fig. 3** Demonstration applications using BiemuS. **(A)** Three structures of cortical  
254 organoids modeled using FS and RS neurons connected with excitatory and inhibitory synaptic  
255 connection (AMPAR and GABA<sub>AR</sub>) based on biological culture observations and their  
256 spiking activity. Synaptic connections are promoted according to rules depending on the  
257 structure to reproduce, spatial placement of neurons and the ratio of inhibition/excitation  
258 connection observed. The spiking activity emulated corresponds to a maximum probability  
259 for connection inside and outside the organoids of respectively 10% and 2% with 512 neurons  
260 per organoid and a 20% inhibition/excitatory neuron ratio. **(B)** Emulation of drug treat-  
261 ment in a single organoid through AMPAR and GABA<sub>AR</sub> full antagonists from 20 seconds  
262 to 40 seconds.

## 263 2.3 Biohybrid experiments

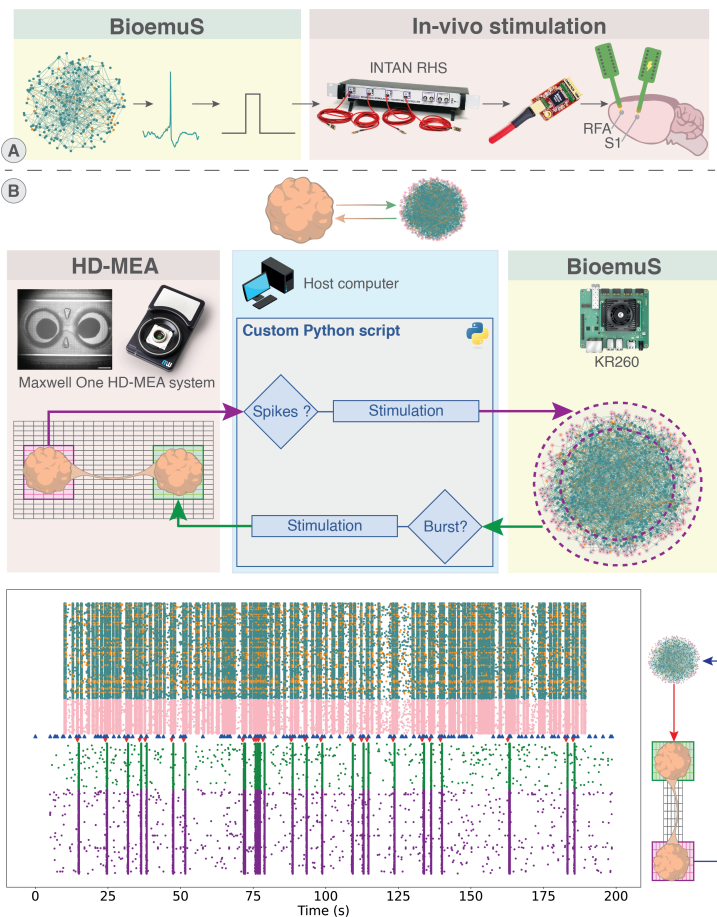
264 This section presents the biohybrid experiments conducted using the system.  
265 It shows how different network implementation from single neuron to larger  
266 network can interact with biology through various interfaces.

### 267 2.3.1 Open loop biomimetic in-vivo stimulation

268 A simple case of interaction with the living thanks to the real-time behav-  
269 ior of BioemuS is to drive open-loop in-vivo stimulation by the SNN [13] as  
270 shown in Figure 4A. This open-loop stimulation was applied to rat brains as a  
271 neuromorphic-based open-loop set-up for neuroprosthetic applications target-  
272 ing post-stroke rehabilitation studies [6, 7]. The spikes from neurons emulated  
273 by BioemuS are output as pulses connected to the INTAN RHS recording/s-  
274 timulation unit to trigger stimulation upon spike reception. The spontaneous  
275 activity of the neurons is tuned to obtain slow or fast activities by tuning  
276 the parameters of the equation ruling the synaptic noise [13]. In this setup,  
277 the latency between spike detection and stimulation is less than a millisecond.  
278 This biohybrid experiment promotes the use of BioemuS as a tool to investi-  
279 gate stroke rehabilitation in an electroceutic approach by providing biomimetic  
280 stimulation.

### 281 2.3.2 Closed-loop biomimetic in-vitro stimulation on high 282 resolution MEA

283 To demonstrate the ease of integration of the system with existing solutions for  
284 biological interfacing as well as its versatility, closed-loop stimulation between  
285 BioemuS and the new generation of HD-MEA (High-Density MicroElectrode  
286 Array)[35] were performed (see Figure 4B). Connected organoids were plated  
287 on HD-MEA. Electrodes were configured to allow activity recording on left  
288 and right organoids while allowing stimulation of the right organoid. A sin-  
289 gle organoid was modeled using BioemuS on a network of 1,024 neurons and  
290 emulating for 180 seconds. Spiking activity of BioemuS was forwarded to the  
291 computer hosting the controlling the HD-MEA system using ZeroMQ over  
292 Ethernet and stimulation was sent using ZeroMQ on the external stimulation  
293 port of BioemuS. A Python script executed on that same computer sent stimu-  
294 lation to the HD-MEA upon receipt of a burst from BioemuS. This experiment  
295 showcases the potential of BioemuS to operate as a tool to study the impact  
296 of adaptive stimulation on a culture following the principles of electroceutics  
297 while highlighting its ability to adapt to a standard biophysical interface. The  
298 benefit of the user-defined model through customizable Python scripts to adapt  
299 to a specific application is also showcased here by assigning XY coordinates to  
300 neurons to take advantage of the spatial resolution provided by the HD-MEA.



301

**Fig. 4** Biohybrid experiments conducted that integrate the system in a biohybrid experimental setup. **(A)** In-vivo stimulation driven by BicemuS spiking activity as a model of post stroke rehabilitation via adaptive stimulation. The spiking activity of the SNN triggers stimulation on an in-vivo culture using the INTAN RHS2116 headstage. Electrode arrays were placed in the rostral forelimb area (RFA) and in the primary somatosensory area (S1) in the brain of adult Long-Evans rats. **(B)** Closed-loop interaction between connected organoids plated on HD-MEA system and single organoid emulated on BioemuS. The spiking activity detected in the left organoid of the connectoid in the last 100ms triggers stimulation on exterior neurons of the emulated single organoid on BioemuS. The bursting activity detected on BioemuS triggers stimulation on the right organoid of the connectoid. Detection and stimulation commands are carried out by Python scripts using. Stimulation on the SNN is performed using the external stimulation slot. BicemuS stimulation triggers are shown by blue triangle and stimulations to HD-MEA by red triangles. BicemuS is running for 180 seconds starting from 10 seconds and synchronize manually with HD-MEA activity based on the first stimulation trigger  $\pm$  300 ms.

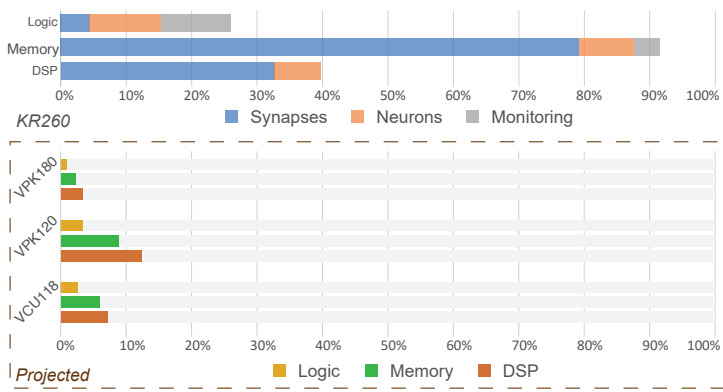
## 317 2.4 Performances

The low-cost platform targeted is the AMD Xilinx Kria KR260 Robotics Starter Kit carrier board embedding the K26 SOM by AMD Xilinx (Zynq

318

319

320 Ultrascale+ MPSoC architecture). This entry level platform is capable of  
321 running 1,024 neurons with 6 conductance-based currents for a total of 2<sup>20</sup>  
322 conductance-based synapses running real-time with a time step of 31.25 µs.  
323 The system can also run on AMD Xilinx Kria KR260 Vision Starter Kit carrier  
324 board with for only restriction the number of PMODs, preventing concurrent  
325 from the concurrent use of DAC waveforms and WiFi spike monitoring. While  
326 most of the memory available is used, less than 50% of the computing capacity  
327 (Logic and Digital Signal Processing slices) of the board is used by the sys-  
328 tem (see Figure 5). As the design is implemented on an entry level target, the  
329 projection of the resources utilization on larger targets suggests the possibility  
330 to run several calculation cores in parallel (see Figure 5) as well as allowing  
331 faster emulation.



332

333 **Fig. 5** Resources utilization of BicemuS. Utilization for main modules implemented on  
334 AMD Xilinx KR260 Robotic Starter Kit and projected on high end evaluation boards from  
335 AMD Xilinx (Versal Premium Series VPK120 and VPK180 Evaluation Kits and Virtex  
336 UltraScale+ VCU118 Evaluation Kit). Logic corresponds to LUT and Flip-Flops, memory  
337 to the total memory implemented as BRAM and URAM, DSP to the number of Digital  
338 Signal Processing (DSP) slices.

339

340

341

342

343

344

345

The average latency observed to send spikes through Zero MQ (UDP) is 240 µs for 100 ms of spiking activity. The average latency observed for spike monitoring through WiFi (UDP) using ESP32 is between 2.8 ms and 6.2 ms depending on the data collection interval. Overall system power consumption is 6.50W with 3.42W associated with the calculation core. Considering only the calculation core that is running on PL part, BicemuS consumes 3.42 times more than SpiNNaker [24] or BrainScaleS-2 [23] that run on ASIC.

346

## 3 Methods

347

### 3.1 SNN modeling

It uses x ionic channels and mimic better different behavior of a cortical neuron. The synapses model is from [Destexhe et al.] and possesses a biophysical

348 12

349

350 explanation on how synapses work. In addition, a synaptic noise using the  
351 ornstein-uhlenbeck process has been used to include spontaneous activities. It  
352 has been proven that such models represent the intrinsic noise present in the  
353 brain [ref]” something like that.

354 The neuron model is based on Hodgkin-Huxley [27] in the Pospischil  
355 paradigm [28] to guarantee biological meaningfulness while limiting resource  
356 consumption and reduce computations. The synapse model used is Destexhe  
357 [31] that describes different type of receptors with a conductance-based model  
358 that provides biological coherence. Synaptic noise is modeled using Orn-  
359 stein-Uhlenbeck process that has been proven to represent the intrinsic noise  
360 present in the brain [29, 30] that allow the system to create spontaneous  
361 activity mimicking biology. The noise seeds are generated by the PS and sent  
362 through AXI LITE to the noise generator thus guarantying true random seeds.  
363 Equations for ionic channel states are computed from pre-calculated rate stored  
364 in memory following the Equation 1 that corresponds to a restated equation  
365 of the forward Euler solving.

366

$$x_{n+1} = r_1(V_n) \times x_n + r_2(V_n). \quad (1)$$

368

369 where,  $x_{n+1}$  and  $x_n$  are respectively the new and current value of the ionic  
370 channel states,  $V_n$  is the membrane voltage at previous time step,  $r_1$  and  $r_2$   
371 are the ion rate tables decoded from membrane voltage.

372 The step and range of the tables are tunable in software but default hard-  
373 ware locks the rate table size to 2048 values (1 BRAM) that provide a good  
374 compromise between accuracy and resource usage. The default range is set to  
375 -76 mV to 52 mV to provide high accuracy for the preset neurons. Temporal  
376 discretization using a small time step compared to the dynamics is chosen to  
377 allow explicit numerical solving with forward Euler.

378

### 379 3.2 FPGA design

380 On PL part, the computation core is clocked at 400 MHz, AXI communica-  
381 tion to PS at 200 MHz and external components on PMOD connectors such as  
382 DAC and ESP32 at 50 MHz. The use of multiple clocks is justified by hardware  
383 limitations of components and blocks, multiple clocking allows all parts of the  
384 design to work close to their maximum to maximize performances. Crossing  
385 clock domain is handled by dual clock BRAM and FIFO for most critical sig-  
386 nals, the remaining signals are either handled by double flip-flops or extended.  
387 The computation core is fully pipelined.

388 Computation of ionic channels states and currents are encoded using 32  
389 bits floating point. It grants good stability and accuracy to the computation of  
390 ionic channels that are critical parts of the neuron dynamics. Since ionic cur-  
391 rents can have different dynamics potentially smaller in comparison to other  
392 currents, floating point coding is more suited for most computation and espe-  
393 cially for multiplications. Calculation of current sum and forward Euler are

393 encoded using 32 fixed point. Large fixed point coding for sum operations  
394 allows to save resources and computation latency compared to floating point,  
395 while guarantying consistent accuracy. The synaptic noise, injection current  
396 and synapses that have less critical accuracy or perform well with fixed-point  
397 coding are computed with 25 and 18 bits fixed point encoding to fit the ranges  
398 of DSP slices. Synaptic weight is coded on 14 bits and can be multiplied by a  
399 factor specified in software to mimic a larger network behavior.  
400

401 The numerical solver used is the explicit forward Euler method  
402 (Euler–Maruyama) with a small time step compared to the system dynamics  
403 to guaranty stability (31.25  $\mu$ s). To maximize performances and limit resources  
404 usage, DSP of the boards were inferred using macros for most operations. The  
405 model is validated using Python implementation emulating both rate table  
406 based computation and fixed point coding.

### 407 3.3 System monitoring and control

The PS part is running the Canonical Ubuntu 22.04 for ZynqMP architecture. The main application controlling the SNN is coded and compiled in C++11. Setup from the PS to the PL is implemented by AXI LITE controlled through /dev/mem in the C++ application.

Communication between the PL to PS is implemented using AXI DMA controlled by the the C++ application using the dma\_proxy driver provided by AMD Xilinx. The application implements a thread for each AXI DMA channel and cyclic buffers for AXI DMA transfers.

The Ethernet communication implements ZeroMQ Push-Pull messaging pattern with a different port for each data (spikes, waveforms, and external stimulation) that can be set from the JSON configuration file.

The interval of data collection can be set from the JSON configuration file from 5ms to 255ms for spike collection *via* DMA, from 3.125 ms to 15 ms for the waveforms collections. The WiFi connection is using UDP protocol and the data collection interval can be set from 2 ms to 20 ms.

The data collection interval for the spikes and waveforms through the DMA directly impacts the load of the application. A small interval will generate more frequent write in file or frame sending thus loading the CPU. The limit corresponds to a data collection interval smaller than the writing or sending time of the frame therefore blocking the software in a thread.

The data collection interval for WiFi forwarding is limited by the hardware and latency of the WiFi protocol so as high interval generates too large buffer and too small interval may generate packet loss.

DMA based monitoring can run local saving and Ethernet forwarding concurrently in most cases with large data collections interval but may dysfunction on small interval due to processor performances. Spikes and waveforms monitoring through DMA can run concurrently in separate threads but may also dysfunction on small data collection intervals due to processor performances. WiFi, DAC and DMA based monitoring can run concurrently without impact on performances. Bash scripts are used to compile the software, update the

437 firmware and launch the application.

439 An external stimulation controlled *via* Ethernet over ZeroMQ allows to send  
440 a stimulation of a given time to a given neuron by passing the stimulation  
441 duration and neuron index to the PL using the AXI DMA.

### 442 3.4 Real-time emulation

443 *Interconnected organoids emulation.* The "single" physically separates the organoids to prevent connection. The "assembloid" or fused places  
444 organoids tens of micrometers apart [32]. The "connectoid" places organoids  
445 centimeters apart while constraining the interconnection to a channel of 150  
446  $\mu\text{m}$  width [33, 34]. The emulation model implements cortical neurons using FS  
447 and RS types connected by AMPAR and GABA<sub>AR</sub>.

448 The synaptic connection rules for the synaptic connections inside organoids  
449 are ruled by Equation 2 that favors connection to neurons close to each other  
450 normalised by the diameter of organoid. The connections between organoids  
451 are ruled by Equation 3 for assembloid and by Equation 4 for connectoid.  
452 The former favors connection to neurons close to each other normalised by  
453 the maximum distance possible between neurons, while the connectoid rule is  
454 promoting connection based on the location of neuron in the organoid that  
455 promotes connection on the exterior ring.

$$457 \quad p_{single} = p_{max} \times \left(1 - \frac{d_{n_{pre}, n_{post}}}{r_{org}}\right) \quad (2)$$

$$462 \quad p_{assembloid} = p_{max} \times \left(1 - \frac{d_{n_{pre}, n_{post}}}{d_{org_{pre}, org_{post}} + r_{org_{pre}} + r_{org_{post}}}\right) \quad (3)$$

$$466 \quad p_{connectoid} = p_{max} \times \frac{1}{2} \times \left(\frac{d_{n_{pre}, org_{pre}}}{r_{org_{pre}}} + \frac{d_{n_{post}, org_{post}}}{r_{org_{post}}}\right) \quad (4)$$

468 where  $p_{max}$  is the maximum probability of connection,  $d$  is the distance,  
469  $diam_{org}$  the diameter of the organoid,  $r$  the radius,  $n_{pre}$  and  $n_{post}$  the pre-  
470 synaptic and post-synaptic neurons,  $org_{pre}$  and  $org_{post}$  the pre-synaptic and  
471 post-synaptic organoids and the distance calculated from the center of the  
472 organoids.

473 *Drug treatment emulation.* The organoid emulated corresponds to 1,024  
474 neurons distributed in 10 % of FS neurons and 90 % of RS neurons. FS neurons  
475 connect with GABA<sub>AR</sub> while RS neurons connect with AMPAR. The synaptic  
476 connections inside the organoids were generated using the same algorithm  
477 as for the single structure (Equation 2). The control of the activation and  
478 inactivation of the synapses is handled by an AXI LITE register that was  
479 set from an external computer using the same port as external stimulation  
480 trigger (Ethernet over ZeroMQ). The python script sending the trigger from  
481 the external computer was designed to disable synaptic connections of BioeS  
482 after 20 seconds of emulation and reactivate after 20 seconds. The python  
483 was synchronized by using a blocking call on the availability of BioemuS to

483 receive frames as it becomes available only after the emulation started. For  
484 the full antagonist AMPAR, the AMPA calculation block was disabled and  
485 the GABA<sub>AR</sub> in the case of the full antagonist GABA<sub>AR</sub>. The activation and  
486 inactivation of the synapses is done by conditional consideration of the synaptic  
487 current in the sum. The spiking activity was recorded using the on-board  
488 saving of spikes with a data collection interval of 100 ms.  
489

### 490 3.5 Biohybrid experiments

491 *Open-loop biomimetic in-vivo stimulation.* The experiment shown in Figure 4A  
492 corresponds to a former version of BioemuS implementing only independent  
493 neurons using exclusively fixed point coding and fitted equations for ionic  
494 channel states based on [36]. The platform was the ZyboZ7-20 running the  
495 C++ application in standalone mode with spike monitoring polled using  
496 AXI LITE and forwarded to the host computer through USB 2.0 CDC. The  
497 parameters of the FS and RS neurons used are the same as in [36]. A spike  
498 was considered in hardware when the membrane potential of a neuron crossed  
499 -10 mV and generated a pulse on a 3.3V digital output. The experiment  
500 conducted corresponds to the work [13] that provides further details on the  
501 experimental setup and protocol.

502 Healthy adult Long-Evans rats (5 male, weight: 300-400g, age: 4-5 months;  
503 Charles River Laboratories, Calco, LC, Italy) were employed for this work.  
504 All the rats were treated with the SNN-based stimulation while they were  
505 deeply anesthetized. The experimental procedures were performed in the  
506 Animal Facility of the Italian Institute of Technology (IIT), Genoa, Italy and  
507 were previously approved by the Italian Ministry of Health and Animal Care  
508 (Italy: authorization n. 509/2020-PR).

509 Anesthesia was induced by placing the rat inside a vaporizing chamber and  
510 injecting gaseous isoflurane (5% @ 1 lpm). The surgical level of anesthesia was  
511 induced by the administration of ketamine (80-100 mg/kg IP) and xylazine  
512 (5-10 mg/kg). The rat was then secured in a stereotaxic frame and all vital  
513 parameters were monitored until the end of the procedure. The surgery began  
514 by applying lidocaine cream (a topical analgesic) before performing a midline  
515 skin incision to expose the skull. Successfully, a laminectomy was performed  
516 at the level of the Cisterna Magna to allow the draining of cerebrospinal fluid  
517 (CSF). Then, based on stereotaxic measurements [9] +3.5, +2.5 and -1.25,  
518 +4.25 AP, ML, burr holes (3 mm diameter) were performed over the primary  
519 somatosensory area (S1) and rostral forelimb area (RFA). Lastly, the dura  
520 mater was removed from the burr holes (RFA and S1) to allow insertion of  
521 MEAs (MEAs; A4x4-5 mm-100-125-703-A16, NeuroNexus)

522 *Closed-loop biomimetically driven stimulation on HD-MEA.* The bi-  
523 directional communication between BioemuS and the HD-MEA system is  
524 ensured by Python scripts running on a gateway computer. The HD-MEA was  
525 configured to record from channels both from left and right organoid based  
526 on an activity scan and to select random stimulation electrodes on the right

527 organoids. The HD-MEA is the MaxOne chip of MaxWell Biosystems AG.  
528 The spikes received from BioemuS on the host computer are analyzed to  
529 detect the presence of a burst in the 100 ms of activity sent. A burst is defined  
530 as more than 64 neurons spiking at least 15 times in the last 100ms. Upon  
531 burst detection, a stimulation of one period of a 100Hz sinus wave with an  
532 amplitude of 40 mV is sent to the HD-MEA using custom Python script based  
533 on manufacturer templates. Stimulation was chosen of amplitude high enough  
534 to allow visualization of the stimulation on the MaxLab Live Software.  
535 The spikes received from the HD-MEA triggered stimulation on BioemuS if at  
536 least 1 spike was detected on at least 2 channels in the last 100ms of activity  
537 collected. The stimulation was sent through Ethernet over ZeroMQ to the  
538 external stimulation port of BioemuS to trigger a stimulation of 6.250ms of  
539 0.03 mA/cm<sup>2</sup> on the neurons on the exterior rings of the organoid.  
540 The Python script implemented executed a thread for each task of receiving  
541 spikes from HD-MEA, receiving spikes from BioemuS, sending stimulation to  
542 Maxwell and sending stimulation to BioemuS.  
543 The activity of the HD-MEA was recording using the MaxLab Live Software  
544 started manually before starting BioemuS. The activity was analysed using  
545 the script provided by the manufacturer. The spiking of activity of BioemuS  
546 was recorded on-board.  
547 The configuration of electrodes of the HD-MEA was exported from the soft-  
548 ware. The XY configuration of neurons, network configuration and stimulated  
549 neurons of BioemuS were exported from the Python scripts. Detection of  
550 burst and spikes triggering stimulation for both HD-MEA and BioemuS were  
551 reconstructed from the recorded data. The synchronization of both activities  
552 was done manually based on the trigger of the first stimulation considering an  
553 approximation of 100 to 300 ms based on the latency of the HD-MEA commu-  
554 nication and the fluctuating latency induced by the Ubuntu operating system.  
555

*Organoid cultures.* Cortical connectoids were generated using previously reported protocol [37]. Briefly, hiPSCs were dissociated using TrypLE Express and 10,000 cells per well were seeded into U-bottom ultra-low attachment 96 well plate (Prime surface, Sumitomo bakelite) in mTeSR plus supplemented with 10µM of Y-23632. 24h later, media was replaced with neural induction media (NIM), consisting of DMEM-F12 with HEPES, 15% (v/v) knockout serum replacement, 1% (v/v) minimal essential media non-essential amino acids (MEM-NEAA), and 1% (v/v) Glutamax, supplemented with 100 nM LDN-193189, 10 µM SB431542, and 5% (v/v) heat-inactivated FBS. On day 2, NIM was replaced without the supplement of FBS and changed every other day until day 10.

From day 10 to 18, culture medium was replaced and changed every other day with neural differentiation media 1 (NDM1), consisting of 1:1 mixture of DMEM/F12 with HEPES and Neurobasal medium, 0.5% (v/v) N2 supplement, 1% (v/v) B27 supplement without vitamin A, 1% (v/v) Glutamax, 0.5%

571 (v/v) MEM-NEAA, 0.25 mg/ml human insulin solution, and 1% (v/v) Peni-  
572 cillin/Streptomycin/Amphotericin (PSA) (Sigma, A5955). On day 18, culture  
573 medium was replaced with neural differentiation media 2(NDM2), consisting  
574 of Neurobasal medium, 0.5% (v/v) N2 supplement, 1% (v/v) B27 supplement  
575 with vitamin A, 1% (v/v) Glutamax, 0.5% (v/v) MEM-NEAA, 0.25 mg/ml  
576 human insulin solution, 200 mM ascorbic acid, and 1% (v/v) PSA, supple-  
577 mented with 20 ng/ml brain derived neurotrophic factor (BDNF). On day 28,  
578 culture media was replaced with Neural Maintenance Media (NMM) consist-  
579 ing of Neurobasal Medium, supplemented with 2% (v/v) B27 supplement with  
580 vitamin A, 1% (v/v) Glutamax, 1% (v/v) PSA and 20 ng/ml BDNF.  
581

582 Cerebral organoids were subjected to connectoid formation after 60 days in  
583 culture. Here, a costume made microfluidic device containing two holes which  
584 are connected through a narrow channel were bonded on a CMOS-based HD-  
585 MEA (MaxOne, Maxwell Biosystems). Microchannel of the microfluidic device  
586 was coated with 2% Matrigel (Corning) in DMEM/F12 for 1h at room tem-  
587 perature (RT). Next, coating solution is replaced with NMM and an organoid  
588 is placed into each of the holes. Cells were kept at 37°C and 5% CO<sub>2</sub> and half  
589 media change was performed every 3-4 days for the duration of cell culture.

## 590 4 Discussion

591 Not applicable.

## 592 5 Conclusion

593 Running a generic operating system on the PS to handle communication offers  
594 versatility and ease integration with existing experimental setups, while reduc-  
595 ing development time where the low-level FPGA development is technical and  
596 time consuming. Another benefit is the ease of use for biologists thanks to the  
597 graphic interface and user-friendly approach offered by an Ubuntu operating  
598 system. While non real-time operating system as Ubuntu induces a discernible  
599 and fluctuating latency, using PL driven interrupt and AXI DMA allows  
600 to obtain relatively low latency about the tens of microseconds. A trade-off  
601 between latency and compatibility/versatility can be found by using solutions  
602 such as data sent directly by PL trough expansion PMODs or ESP32, real-  
603 time operating system or running the application the real-time cores of the  
604 chip. Nonetheless, direct monitoring on the PL that drastically reduces the  
605 latency remains possible using the various connectors of the board but at the  
606 cost of longer and more complex development.

On the current target, the main bottleneck lies in the memory usage  
essentially allocated for synapses weights and pre-calculated ionic channel  
states. Since the current target is using a preceding architecture, more efficient  
architectures of memory can be found in recent larger targets such as High  
Bandwidth Memory (HBM) that integrates DRAM directly into the FPGA  
package, thus providing drastically higher depth and bandwidth. Latest AMD  
Xilinx chips also incorporate adaptive SoCs that provide significantly higher

612 18

613 computation power notably with native floating point DSP and AI engine  
614 while still embedding a Zynq for setup and control Figure 5. Hence porting a  
615 similar architecture of SNN on these targets would significantly increase per-  
616 formances and create a *viable* alternative to standard GPU. An alternative  
617 would be to reduce the number of synapses as fully connected network is not  
618 always necessary, thus allowing the implementation of more neurons.

619  
620 The system has proven its ease of integration demonstrated by the biohy-  
621 brid experiments conducted on most widespread biophysical interface where  
622 low-level communication protocol (pulse on digital output) as well as complex  
623 communication protocols (WiFi and Ethernet) were implemented. The ease of  
624 use also has been particularly promoted by the application Figure 3A showing  
625 an example of complex network could be created simply from a customizable  
626 Python script. The experiment in Figure 4B also highlighted this feature by  
627 interfacing the BioemuS to a biophysical interface using only Python scripts.

628  
629 The presented applications demonstrate the flexibility of BioemuS in adapt-  
630 ing to the study of various biological processes, including stroke trough in-vivo  
631 stimulation (see Figure 4A) and the potential for neuroprostheses replacement  
632 through closed-loop in-vitro stimulation driven by BioemuS (see Figure 4B).

633 We are proposing a low-cost, flexible and real-time biomimetic tool that  
634 could allow wider exploration of the mechanism of the living thanks to real-  
time emulation and hybridization.

635 **Supplementary information.** Not applicable.

636 **Acknowledgments.** We acknowledge Landry Bailly for the synaptic con-  
637 nection heatmap of the organoid emulation, Andréa Combette for the analysis  
638 of the spiking activity of the organoid emulation, Mattia Di Florio and Marta  
639 Carè for the preparation and execution of the experiment on open-loop in-vivo  
640 stimulation. We also acknowledge Ryota Murai for his advice on the RedPi-  
641 taya system, Hu Huaruo and Atsuhiro Nabeta for their advice and assistance  
642 on the data acquisition from Maxwell system.

## 643 **Declarations**

### 644 **Funding**

645 This work was supported by IdEx International of University of Bordeaux  
646 and the JSPS Core-to-Core Program (grant number:JPJSCCA20190006). This  
647 work was also supported by the Institute for AI and Beyond.

### 648 **Competing interests**

649 The authors declare no competing interests.

### 650 **Ethics approval**

651 Not applicable.

652 **Consent to participate**

653 Not applicable.

654 **Consent for publication**

655 Not applicable.

656 **Availability of data and materials**

657 The data analysed in this study are available from the corresponding authors  
658 upon reasonable request.

659 **Code availability**

660 The code related to the experiments and tests is available from the correspond-  
661 ing authors upon reasonable request.

662 **Author contributions**

663 R.B. designed both the software and hardware part of the system, developed  
664 the Python scripts, performed the biohybrid experiments, analysed the results  
665 and wrote the manuscript. J.C. participated in the development of the hard-  
666 ware design of the synapses, WiFi communication on ESP32 and designed the  
667 reduced version controlling snake robot. T.D. cultivated the organoids, per-  
668 formed the analysis of the data from the Maxwell system and captured the  
669 images of the cultures. F.K. participated in the design of the reduced version  
670 working controlling the snake robot. T.L. supervised and participated in the  
671 design of the applications and biohybrid experiments. Y.I. and P.B. supervised  
672 and advised on the biohybrid experiments and biological modeling. T.L., Y.I.  
673 and P.B joined the discussion and corrected the draft manuscript. All authors  
674 discussed and revised the final manuscript.

675 **Appendix A Section title of first appendix**

676 **References**

- 677 [1] Organization, W.H., et al.: The top 10 causes of death; 24 May 2018  
678 (2020)
- 679 [2] Chin, J.H., Vora, N.: The global burden of neurologic diseases. Neurology  
680 **83**(4), 349–351 (2014)
- 681 [3] French, B., Thomas, L.H., Coupe, J., McMahon, N.E., Connell, L., Har-  
682 rison, J., Sutton, C.J., Tishkovskaya, S., Watkins, C.L.: Repetitive task  
683 training for improving functional ability after stroke. Cochrane database  
684 of systematic reviews (11) (2016)

- 685 [4] Farina, D., Vujaklija, I., Bränemark, R., Bull, A.M., Dietl, H., Graimann,  
686 B., Hargrove, L.J., Hoffmann, K.-P., Huang, H., Ingvarsson, T., et al.:  
687 Toward higher-performance bionic limbs for wider clinical use. *Nature  
688 biomedical engineering*, 1–13 (2021)
- 689 [5] Bouton, C.E., Shaikhouni, A., Annetta, N.V., Bockbrader, M.A., Frieden-  
690 berg, D.A., Nielson, D.M., Sharma, G., Sederberg, P.B., Glenn, B.C.,  
691 Mysiw, W.J., et al.: Restoring cortical control of functional movement in  
692 a human with quadriplegia. *Nature* **533**(7602), 247–250 (2016)
- 693 [6] Panuccio, G., Semprini, M., Natale, L., Buccelli, S., Colombi, I., Chiap-  
694 palone, M.: Progress in neuroengineering for brain repair: New challenges  
695 and open issues. *Brain and neuroscience advances* **2**, 2398212818776475  
696 (2018)
- 697 [7] Semprini, M., Laffranchi, M., Sanguineti, V., Avanzino, L., De Icco, R.,  
698 De Micheli, L., Chiappalone, M.: Technological approaches for neuroreha-  
699 bilitation: from robotic devices to brain stimulation and beyond. *Frontiers  
700 in neurology* **9**, 212 (2018)
- 701 [8] Famm, K., Litt, B., Tracey, K.J., Boyden, E.S., Slaoui, M.: A jump-start  
702 for electroceuticals. *Nature* **496**(7444), 159–161 (2013)
- 703 [9] Reardon, S., et al.: Electroceuticals spark interest. *Nature* **511**(7507), 18  
704 (2014)
- 705 [10] Christensen, D.V., Dittmann, R., Linares-Barranco, B., Sebastian, A.,  
706 Le Gallo, M., Redaelli, A., Slesazeck, S., Mikolajick, T., Spiga, S., Menzel,  
707 S., et al.: 2022 roadmap on neuromorphic computing and engineering.  
708 *Neuromorphic Computing and Engineering* **2**(2), 022501 (2022)
- 709 [11] Xu, T., Xiao, N., Zhai, X., Chan, P.K., Tin, C.: Real-time cerebellar  
710 neuroprosthetic system based on a spiking neural network model of motor  
711 learning. *Journal of Neural Engineering* **15**(1), 016021 (2018)
- 712 [12] Sharifshazileh, M., Burelo, K., Sarnthein, J., Indiveri, G.: An electronic  
713 neuromorphic system for real-time detection of high frequency oscillations  
714 (hfo) in intracranial eeg. *Nature communications* **12**(1), 3095 (2021)
- 715 [13] Di Florio, M., Carè, M., Beaubois, R., Barban, F., Levi, T., Chiappalone,  
716 M.: Design of an experimental setup for delivering intracortical micro-  
717 stimulation in vivo via spiking neural network. In: 2023 45th Annual  
718 International Conference of the IEEE Engineering in Medicine & Biology  
719 Society (EMBC) (2023). IEEE
- 719 [14] Corradi, F., Indiveri, G.: A neuromorphic event-based neural record-  
ing system for smart brain-machine-interfaces. *IEEE transactions on*

720

721

722 biomedical circuits and systems **9**(5), 699–709 (2015)

723 [15] Hines, M.L., Carnevale, N.T.: Neuron: a tool for neuroscientists. The  
724 neuroscientist **7**(2), 123–135 (2001)

725 [16] Gewaltig, M.-O., Diesmann, M.: Nest (neural simulation tool). Scholar-  
726 pedia **2**(4), 1430 (2007)

727 [17] Stimberg, M., Brette, R., Goodman, D.F.: Brian 2, an intuitive and  
728 efficient neural simulator. Elife **8**, 47314 (2019)

729 [18] Van Albada, S.J., Rowley, A.G., Senk, J., Hopkins, M., Schmidt, M.,  
730 Stokes, A.B., Lester, D.R., Diesmann, M., Furber, S.B.: Performance  
731 comparison of the digital neuromorphic hardware spinnaker and the neu-  
732 ral network simulation software nest for a full-scale cortical microcircuit  
733 model. Frontiers in neuroscience **12**, 291 (2018)

734 [19] Tavanaei, A., Ghodrati, M., Kheradpisheh, S.R., Masquelier, T., Maida,  
735 A.: Deep learning in spiking neural networks. Neural networks **111**, 47–63  
736 (2019)

737 [20] Donati, E., Payvand, M., Risi, N., Krause, R., Indiveri, G.: Discrimination  
738 of emg signals using a neuromorphic implementation of a spiking neural  
739 network. IEEE transactions on biomedical circuits and systems **13**(5),  
740 795–803 (2019)

741 [21] Davidson, S., Furber, S.B.: Comparison of artificial and spiking neu-  
742 ral networks on digital hardware. Frontiers in Neuroscience **15**, 651141  
743 (2021)

744 [22] Merolla, P., Arthur, J.V., Alvarez-Icaza, R., Cassidy, A.S., Sawada, J.,  
745 Akopyan, F., Jackson, B.L., Esser, S.K., Appuswamy, R., Taba, B., Amir,  
746 A., Flickner, M.: Merolla communication network and interface a million  
747 spiking-neuron integrated circuit with a scalable. (2014)

748 [23] Pehle, C., Billaudelle, S., Cramer, B., Kaiser, J., Schreiber, K., Strad-  
749 mann, Y., Weis, J., Leibfried, A., Müller, E., Schemmel, J.: The  
750 brainscales-2 accelerated neuromorphic system with hybrid plasticity.  
751 Frontiers in Neuroscience **16** (2022)

752 [24] Painkras, E., Plana, L.A., Garside, J., Temple, S., Galluppi, F., Patterson,  
753 C., Lester, D.R., Brown, A.D., Furber, S.B.: Spinnaker: A 1-w 18-core  
754 system-on-chip for massively-parallel neural network simulation. IEEE  
755 Journal of Solid-State Circuits **48**(8), 1943–1953 (2013)

[25] Davies, M., Srinivasa, N., Lin, T.-H., Chinya, G., Cao, Y., Choday, S.H.,  
Dimou, G., Joshi, P., Imam, N., Jain, S., *et al.*: Loihi: A neuromorphic

- 756 manycore processor with on-chip learning. *Ieee Micro* **38**(1), 82–99 (2018)
- 757
- 758 [26] Stradmann, Y., Billaudelle, S., Breitwieser, O., Ebert, F.L., Emmel, A.,  
759 Husmann, D., Ilmberger, J., Müller, E., Spilger, P., Weis, J., *et al.*: Demonstrating  
760 analog inference on the brainscales-2 mobile system. *IEEE Open Journal of Circuits and Systems* **3**, 252–262 (2022)  
761
- 762
- 763 [27] HODGKIN, A., HUXLEY, A.: A quantitative description of membrane  
764 current and its application to conduction and excitation in nerve. *Bulletin  
765 of Mathematical Biology* **52**(1-2), 25–71 (1990). [https://doi.org/10.1016/s0092-8240\(05\)80004-7](https://doi.org/10.1016/s0092-8240(05)80004-7)  
766
- 767 [28] Pospischil, M., Toledo-Rodriguez, M., Monier, C., Piwkowska, Z., Bal,  
768 T., Frégnac, Y., Markram, H., Destexhe, A.: Minimal Hodgkin-Huxley  
769 type models for different classes of cortical and thalamic neurons. *Biological Cybernetics* **99**(4-5), 427–441 (2008). <https://doi.org/10.1007/s00422-008-0263-8>  
770
- 771
- 772 [29] Destexhe, A., Rudolph, M., Fellous, J.M., Sejnowski, T.J.: Fluctuating  
773 synaptic conductances recreate in vivo-like activity in neocortical  
774 neurons. *Neuroscience* **107**(1), 13–24 (2001). [https://doi.org/10.1016/S0306-4522\(01\)00344-X](https://doi.org/10.1016/S0306-4522(01)00344-X)  
775
- 776 [30] Grassia, F., Kohno, T., Levi, T.: Digital hardware implementation  
777 of a stochastic two-dimensional neuron model. *Journal of Physiology  
778 Paris* **110**(4), 409–416 (2016). <https://doi.org/10.1016/j.jphysparis.2017.02.002>  
779
- 780 [31] Destexhe, A., Mainen, Z.F., Sejnowski, T.J.: Kinetic models of synaptic  
781 transmission: From Ions to Networks. *Methods in Neural Modeling: from  
782 Ions to Networks*, 1–25 (1998)
- 783 [32] Pașca, S.P.: Assembling human brain organoids. *Science* **363**(6423), 126–  
784 127 (2019)
- 785 [33] Kirihara, T., Luo, Z., Chow, S.Y.A., Misawa, R., Kawada, J., Shibata, S.,  
786 Khooyratee, F., Vollette, C.A., Volz, V., Levi, T., *et al.*: A human induced  
787 pluripotent stem cell-derived tissue model of a cerebral tract connecting  
788 two cortical regions. *Iscience* **14**, 301–311 (2019)
- 789 [34] Kawada, J., Kaneda, S., Kirihara, T., Maroof, A., Levi, T., Eggan, K.,  
790 Fujii, T., Ikeuchi, Y.: Generation of a motor nerve organoid with human  
791 stem cell-derived neurons. *Stem cell reports* **9**(5), 1441–1449 (2017)
- 792
- 793 [35] Ballini, M., Müller, J., Livi, P., Chen, Y., Frey, U., Stettler, A., Shad-  
794 mani, A., Viswam, V., Jones, I.L., Jäckel, D., *et al.*: A 1024-channel cmos  
795 microelectrode array with 26,400 electrodes for recording and stimulation

792

793

794

795

796

23

of electrogenic cells in vitro. IEEE journal of solid-state circuits **49**(11),  
2705–2719 (2014)

[36] Khooyratee, F., Grassia, F., Saïghi, S., Levi, T.: Optimized real-time  
biomimetic neural network on fpga for bio-hybridization. Frontiers in  
neuroscience **13**, 377 (2019)

[37] Osaki, T., Ikeuchi, Y.: Advanced complexity and plasticity of neural activi-  
ty in reciprocally connected human cerebral organoids. BioRxiv, 2021–02  
(2021)

802